Structural trends in amorphous carbon

C. Z. Wang and K. M. Ho
Ames Laboratory and Department of Physics, Iowa State University, Ames, Iowa 50011
(Received 14 June 1994)

Amorphous carbon (a-C) structures over a wide range of densities are generated using tight-binding molecular-dynamics simulations. The a-C networks obtained by quenching low-density liquids consist of mostly threefold coordinated atoms. These a-C structures correspond to those obtained experimentally by evaporation or sputtering of graphite. However, the a-C networks generated by quenching high-density liquids are found to be dominated by tetrahedral bonding sites, which resemble the diamondlike a-C films produced by the mass-selected ion beam deposition technique. Our study shows that the shape and position of the first peak of the radial distribution function in a-C are very sensitive to the relative concentration of sp, sp^2, and sp^3 bondings. The peak position shifts towards larger distance as the percentage of the fourfold sites increases, which gives a good indication of the relative population of threefold to fourfold sites in the system.

I. INTRODUCTION

The extraordinary ability of carbon atoms to form strong chemical bonds in twofold (linear chain), threefold (graphite), and fourfold (diamond) coordinated structures makes the disordered phase of carbon very complex and fascinating. While amorphous carbon (a-C) films produced by evaporation or sputtering of graphite consist of mostly threefold atoms, those generated by mass-selected ion beam (MSIB) deposition technique are found to be dominated by diamondlike tetrahedral sp^3 bonded sites.[1–5] This unique bonding nature in a-C has attracted considerable technological as well as fundamental interests.[1] In the last several years, extensive experimental investigations involving neutron scattering,[2,4] electron diffraction,[3] electron energy loss spectroscopy,[5] and theoretical studies using computer simulations[6–15] have been devoted to elucidating the microscopic structure and bonding nature of this disordered form of carbon. While these studies did provide many useful data about the structure of a-C, the microscopic bonding nature in this novel material is still not well understood. Even the most basic information such as the relative concentration of various coordinated atoms in the a-C structure is still controversial in the literature.

In this paper, we present a comprehensive report on tight-binding molecular-dynamics (TBMD) simulation studies of the microscopic structures of a-C covering a wide range of densities from the low-density to the high-density regime. Our purpose is to understand the atomistic configurations and structural trend in a-C samples prepared under different conditions. Our simulation results show that the concentration and distribution of various coordinated atoms in a-C samples are very dependent on the sample preparation conditions. The general trend is that the fraction of fourfold coordinated sites increases with increasing sample densities. The sp^3 bonding becomes dominant when the density approaches the density of diamond. Our studies also show that the shape and the peak position of the radial distribution function are strongly correlated with the relative concentration of twofold, threefold, and fourfold coordinated atoms in the a-C samples.

This paper is arranged as follows: Section II describes details of the simulation method and the a-C sample preparation procedures. The structural properties of the a-C samples obtained from our simulations are presented and discussed in Secs. III and IV. Brief concluding remarks are given in the final section.

II. SIMULATION METHOD

In TBMD simulations, the atomic motions are governed by the following Hamiltonian:

$$H(\{\mathbf{r}_i\}) = \sum_i \frac{\mathbf{P}_i^2}{2m} + \sum_n^{\text{occupied}} \langle\psi_n|H_{\text{TB}}(\{\mathbf{r}_i\})|\psi_n\rangle + E_{\text{rep}}(\{\mathbf{r}_i\}) , \quad (1)$$

where $\{\mathbf{r}_i\}$ denotes the positions of the atoms ($i = 1, 2, ..., N$), and $\mathbf{P}_i$ denotes the momentum of the ith atom. The first term in (1) is the kinetic energy of the ions, the second term is the electronic band-structure energy calculated from a parametrized tight-binding Hamiltonian $H_{\text{TB}}(\{\mathbf{r}_i\})$, and the third term is a short-ranged repulsive energy. In this scheme, the quantum mechanical nature of the covalent bonding among the carbon atoms is taken into account explicitly in the electronic structure which is calculated for each of the atomic configurations in the MD simulations. Electronic degrees of freedom are explicitly involved in the force calculation but not in the dynamics. The former feature places the scheme within the quantum mechanics regime, while the latter allows the simulation to have time steps similar to those in traditional molecular-dynamics simulations.

The tight-binding potential model used in the present TBMD simulation describes accurately the energetic, vibrational, and elastic properties of the diamond

(fourfold), graphite (threefold), and linear-chain structures (twofold), in comparison with self-consistent first-principles density functional calculations.[16] We have also calculated the energy barrier for diamond to rhombohedral graphite transition along the path proposed in the previous work of Fahy and Louie.[17] The energy barrier obtained by our TB model is 0.27 eV/atom, compared to the self-consistent density functional calculation result of 0.33 eV/atom.[17] The model has been successfully applied to studies of carbon fullerenes,[18] liquid, and amorphous carbon phases.[10,11,19] Details of the tight-binding model for carbon and the tight-binding molecular-dynamics scheme have been given in our previous publications.[16,21]

In this paper, a-C samples are generated by quenching high temperature carbon liquids of various densities. The simulations are performed with 216 atoms in a cubic cell with periodic boundary conditions. Only the Γ point is used for the electronic structure calculations. The MD time step is 1.05×10^{-15} s. Initially, the liquid carbon samples with densities of 2.20, 2.44, 2.68, 3.0, 3.5, 4.0, and 4.4 g/cm^3, respectively, are equilibrated at high temperatures (6000 K for the samples with densities equal to or below 3.0 g/cm^3, 10 000 K for the samples of 3.5 and 4.0 g/cm^3, and 14 000 K for the sample of 4.4 g/cm^3). The stochastic temperature control method[20] is used to quench the liquids down to 0 K with a cooling rate of about 500 K/ps. (The effects of cooling rate are also studied and will be discussed at the end of the next section.) The volume and shape of the MD cell are kept unchanged in the quenching process. The as-quenched samples are then relaxed to a local energy minimum and zero pressure by a steepest-descent procedure. We found that the as-quenched structures of the four lower-density samples are already very close to the local energy minimum and zero-pressure configuration, while the densities of the three higher-density samples have to be relaxed to 3.30, 3.35, and 3.40 g/cm^3, respectively, in order to reach the local energy minimum. The relaxed networks of these three higher-density samples are then subjected to a reannealing cycle for another 6 ps. In the reannealing process, the temperature of the system was raised to 2500 K and then cooled down to 0 K. After relaxation and reannealing, the structures of the four lower-density samples change very little, while the concentraction of the fourfold atoms in the three higher-density samples decreases by 6% (for samples E and F) and 3% (for sample G), respectively. All results presented in the following two sections are those obtained after relaxation and reannealing procedures.

III. SIMULATION RESULTS

A. Radial distribution functions

The pair-correlation functions of the a-C samples at various densities obtained from our simulations are plotted in Fig. 1. Each spectrum has been averaged over 2000 MD steps at a temperature of 700K. This temperature is comparable with the experimental condition of room temperature if one includes the effects of zero-point-motion of the carbon atoms.[22] The most striking feature of this plot is that the positions of the first peak of the pair-correlation functions shift systematically towards larger distance as the density of the sample is increased. This unusual behavior is found to originate from the increase in the concentration of fourfold atoms in the a-C samples, as one can see from Fig. 2 and Table I, where the relative concentrations of the two-, three-, and fourfold coordinated sites in the a-C samples are presented. A coordination radius of 1.93 Å, which corresponds to the minimum between the first and second peaks in the radial distribution function, is used here to determine the coordination number of each site. We also examined the bond-length distribution corresponding to twofold, threefold, and fourfold atoms in a-C samples at various densities and found that the bond-length distributions are not very sensitive to the density of the sample but depend strongly on the bonding topologies (i.e.,

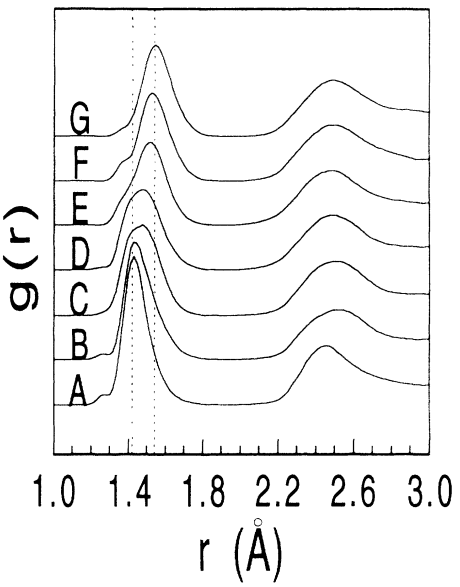

FIG. 1. The pair-correlation functions of the a-C samples generated under various densities as specified in Table I. Note that the first peak position shifts systematically toward larger bond lengths as the density increases. The two dashed vertical lines indicate the bond length of graphite (1.42 Å) and diamond (1.54 Å), respectively.

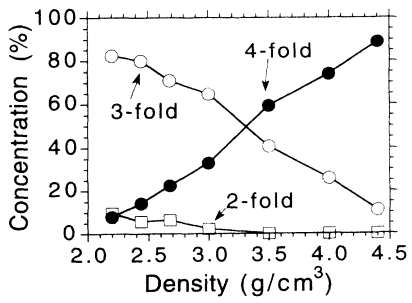

FIG. 2. The concentration of various coordinated atoms in the a-C samples as a function of quenching density.

TABLE I. Concentration of various coordinated atoms in the amorphous carbon networks. Both quenching density and the final equilibrium density (in the parenthesis) are shown for each sample. The table also shows the binding energies of the a-C samples (relative to that of diamond).

Sample	Density (g/cm^3)	Twofold (%)	Threefold (%)	Fourfold (%)	Energy (eV/atom)
A	2.20 (2.20)	9.7	82.4	7.9	+0.6579
B	2.44 (2.44)	5.8	80.0	14.2	+0.6527
C	2.68 (2.68)	6.5	71.0	22.5	+0.6551
D	3.00 (3.00)	2.3	64.7	33.0	+0.5788
E	3.50 (3.30)	0.0	40.7	59.3	+0.4943
F	4.00 (3.35)	0.0	26.0	74.0	+0.5404
G	4.40 (3.40)	0.0	11.0	89.0	+0.5328

twofold, threefold, or fourfold) of the atoms. This result can be seen from Fig. 3 where the first peaks of the partial pair-correlation functions g_{22}, g_{33}, and g_{44} in the a-C samples of various densities are plotted. Since the distance between the fourfold atoms is the longest, it is expected that samples with larger percentages of fourfold atoms will have larger average bond lengths.

B. Angular distribution functions

Figure 4 shows the bond-angle distribution functions in the a-C networks at various densities. At low densities, the angle distributions are quite broad with peaks at about 118°, which is close to the graphitic bond angle of 120°. There are also some large bond angles which are mostly related to the twofold atoms in the network. The center of the bond-angle distribution function shifts toward the tetrahedral bond angle as the fourfold concentration in the a-C networks increases. The bond angles of the two diamondlike a-C networks (samples F and G) are distributed around 109°, close to the tetrahedral bond angle. The root-mean-square (RMS) value of the bond-angle distributions at the fourfold sites in the two diamondlike a-C samples are found to be about 10.5°, similar to the case of amorphous Si, where the RMS bond-angle distribution is about 10°.[23]

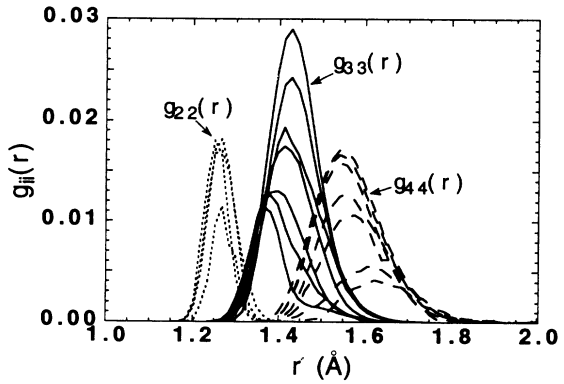

FIG. 3. The partial pair-correlation functions in the a-C samples as specified in Table I. The intensities of the spectra have been divided by the number of atoms of different coordinations, respectively. Note that the peak positions of $g_{22}(r)$, $g_{33}(r)$, and $g_{44}(r)$ are well separated.

C. Ring statistics

In addition to the radial and angular distribution functions, the structures of the amorphous networks have also been characterized by a ring statistics analysis. We compute the ring populations in each a-C sample by the "shortest-path" ring algorithm proposed by Franzblau.[24] The results are shown in Fig. 5. In the low-density samples, in addition to the five-, six-, and seven-membered rings which arise primarily from clusters of threefold atoms, there is a notable number of rings with sizes between 10 and 16. These medium-sized rings are primarily due to the presence of small voids between the threefold clusters in the low-density a-C networks. As the density is increased, the small voids disappear gradually, and at the same time the population of the six-membered rings increases rapidly due to the growth of fourfold diamondlike domains. The ring populations of the two high-density samples are very similar to that of a-Si, which is consistent with the formation of tetrahedral networks.

D. Atomic configurations

The atomistic structures of several a-C samples obtained from our TBMD simulations are shown in Fig. 6. The pictures clearly show that the population of the threefold atoms decreases while that of fourfold atoms increases as the density at which the a-C sample is prepared increases. The tendency of segregation of three-

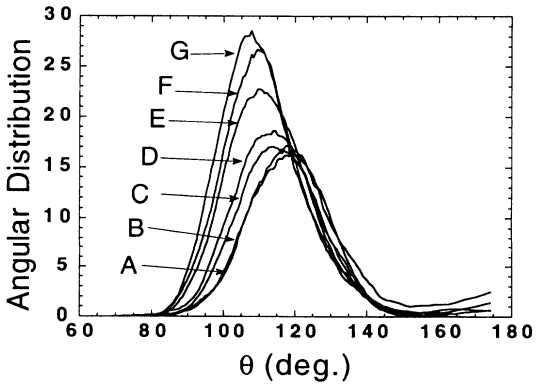

FIG. 4. The bond-angle distribution functions in the a-C samples as specified in Table I.

fold and fourfold atoms is observed in both low-density sp^2-dominated samples as well as in high-density sp^3-dominated samples. The threefold coordinated atoms in the low-density (2.20 and 2.44 g/cm^3) a-C samples are found to form large clusters which are linked together by two- and fourfold atoms. As the density increases, the threefold clusters shrink in size while the "bridge" regions expand and are increasingly dominated by fourfold atoms which also tend to form clusters. The a-C structures obtained by quenching from highly compressed liquids are found to contain mostly fourfold atoms.

E. Effects of quenching rate

We studied the effects of quenching procedures on the final structures of a-C samples by comparing two samples generated under the same density but with different quenching rates. In the low-density regime, we generate two samples under a density of 2.20 g/cm^3 but with a simulation time of 25 and 11 ps, respectively, for quenching and annealing. In the high-density regime, we compare two structures generated from the liquid of 4.0 g/cm^3, with quenching rates of 500 K/ps and 1000 K/ps, respectively. The structures of both as-quenched high-density a-C networks are finally relaxed to a density of 3.35 g/cm^3 and reannealed for another 6 and 3 ps, respectively, up to a temperature of 2500 K.

In Tables II and III and in Figs. 7–10, we compare the relative concentrations of various coordinated atoms, the radial distribution functions, and the angular distribution functions of the a-C structures generated at the same density but with different annealing procedures as discussed in the previous paragraph. The results show that the essential features and bond topologies of the a-C generated under the same density are very similar, suggesting that the structural trend in a-C as discussed above is valid even with longer simulation time. Nevertheless, our simulation results also show that the final structures from different simulation procedures differ in some details. In the low-density samples, the concentration of the various coordinated atoms is slightly different (about a few percent). In the two high-density samples, although the sp^3 to sp^2 ratios coincide with each other, the details of the atomic configurations are different. In particular, the 58 threefold atoms in the sample with longer simulation time consist of one isolated threefold atom (dangling bond), six pairs of atoms, one C_3 chain, five C_4 chains, and a large cluster of 22 atoms, while the threefold atoms in another sample are distributed in the form of relative smaller clusters: one C_{10}, two C_8, one C_6, two C_4, and nine isolated pairs of atoms. Since the electronic states around the Fermi level produced by different sizes of sp^2 clusters in the a-C structures are very different,[25] we expect that the electronic structures of a-C near the gap region will also be sensitive to the sample preparation procedures.

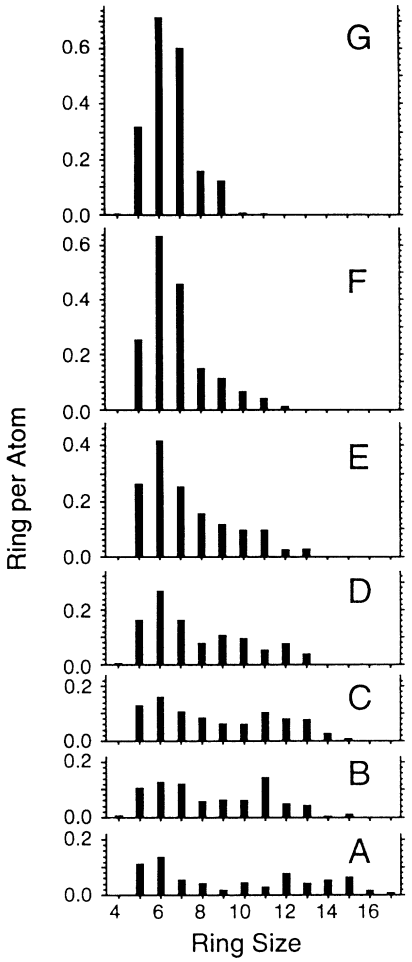

FIG. 5. Populations of the "shortest-path" rings (per atom) in the a-C samples as specified in Table I.

IV. DISCUSSIONS

A. Low-density a-C

The structural properties of low-density sp^2-dominated a-C have been studied extensively by computer simula-

TABLE II. Concentration of various coordinated atoms in the amorphous carbon networks generated under a density of 2.20 g/cm^3 but with different quenching rates. Sample A is the structure obtained with longer simulation time. Both quenching density and the final equilibrium density (in the parenthesis) are shown for each sample. The table also shows the binding energies of the samples (relative to that of diamond).

Sample	Density (g/cm^3)	Twofold (%)	Threefold (%)	Fourfold (%)	Energy (eV/atom)
A	2.20 (2.20)	9.7	82.4	7.9	+0.6579
A'	2.20 (2.20)	12.0	80.6	7.4	+0.6876

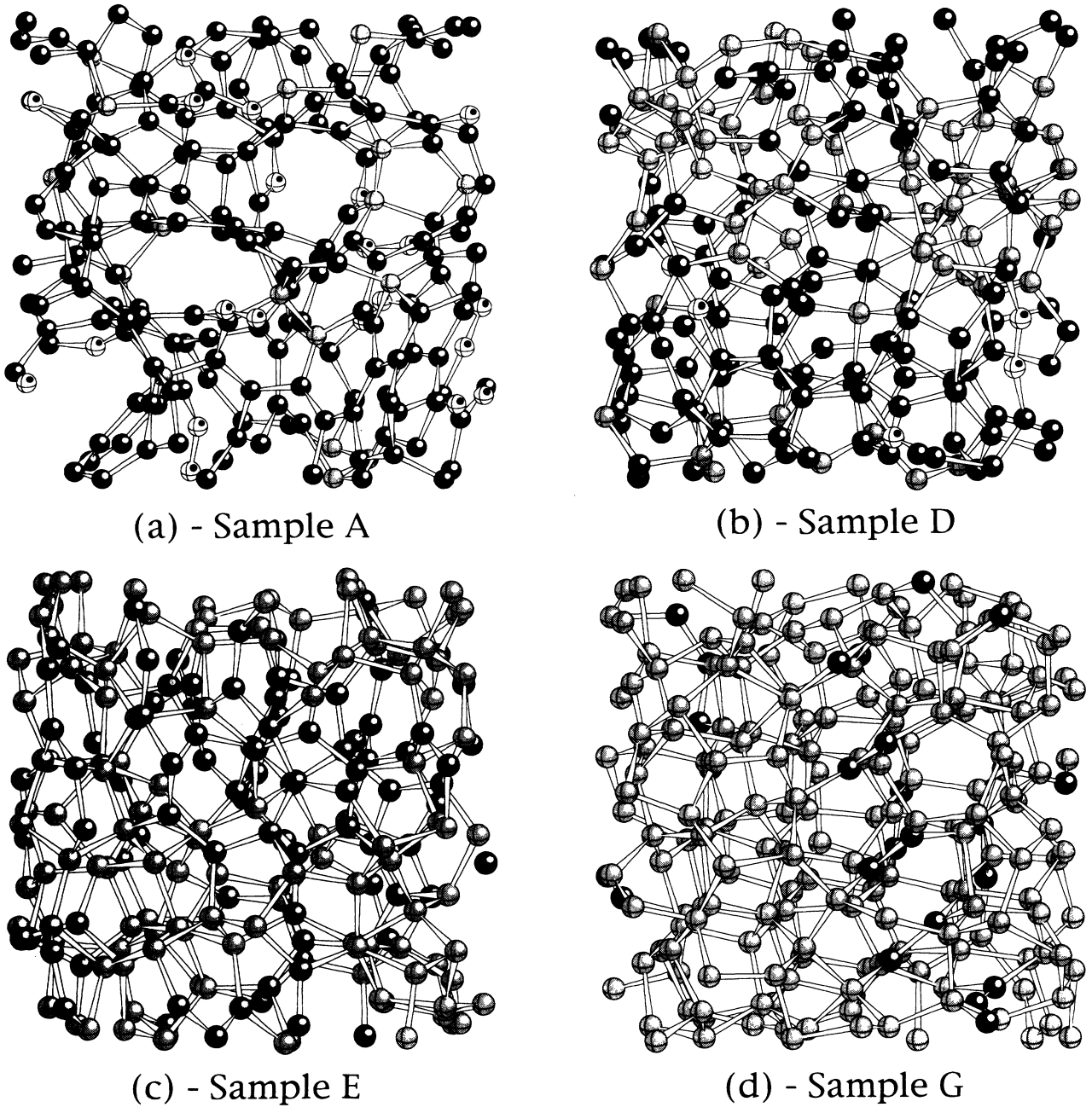

FIG. 6. Microscopic structure of the TBMD-generated a-C networks. (a) sample A, (b) sample D, (c) sample E, and (d) sample G. The different shadings represent different coordinations for the atomic sites (twofold, white balls with small dark dots; threefold, dark shaded balls; fourfold, light shaded balls).

TABLE III. Concentration of various coordinated atoms in the amorphous carbon networks generated under a density of 4.0 g/cm^3 but with different quenching rates. Sample F is the structure obtained with longer simulation time. Both quenching density and the final equilibrium density (in the parenthesis) are shown for each sample. The table also shows the binding energies of the samples (relative to that of diamond).

Sample	Density (g/cm^3)	Twofold (%)	Threefold (%)	Fourfold (%)	Energy (eV/atom)
F	4.00 (3.35)	0.0	26.0	74.0	+0.5404
F'	4.00 (3.35)	0.0	26.0	74.0	+0.5559

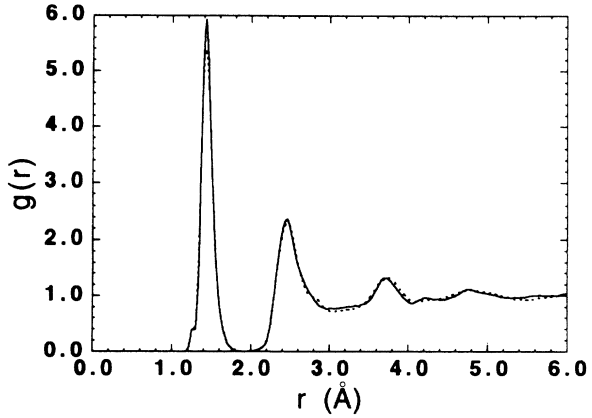

FIG. 7. Pair-correlation functions of the two amorphous carbon networks generated under a density of 2.20 g/cm^3 but with different quenching rates. The solid line represents the result from the sample obtained with longer simulation time.

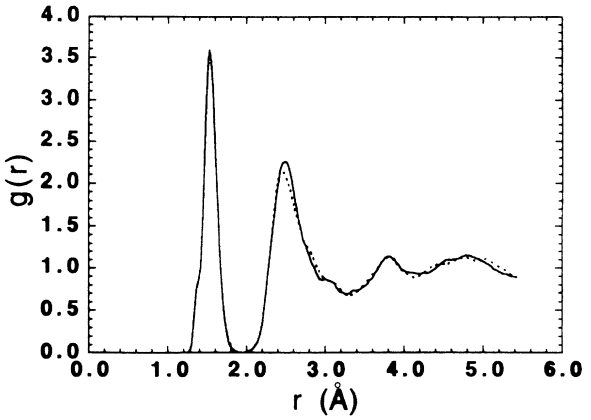

FIG. 9. Pair-correlation functions of the two amorphous carbon networks generated under a density of 4.00 g/cm^3 but with different quenching rates. The solid line represents the result from the sample obtained with longer simulation time.

tions[6–8,14] and by neutron scattering measurement.[2] It was shown by Li and Lannin that although previous theoretical a-C models reproduce some of the features, they did not describe accurately the radial distribution function obtained from neutron scattering experiments.[2] In comparison, our present results show much better agreement with the experimental data. In Fig. 11, we compare the results of the radial distribution function $T(r)$ obtained from our TBMD simulation with that of neutron scattering data of Ref. 2. We choose our results at the density of 2.20 g/cm^3, given that the density of the experimental sample was estimated to be between 2.0 and 2.44 g/cm^3. From Fig. 11, one sees that our model gives a much better description of the experimental radial distribution function than the other theoretical models quoted in Ref. 2. In addition, the percentage of fourfold sites found in our simulation results is also in good agreement with the value of 6.5±1.5 % estimated by a nuclear magnetic resonance (NMR) study[26] of the same a-C sample used in the neutron scattering measurement.

It is worth noting that a certain number of twofold coordinated atoms are present in our low-density a-C samples. Two-fold atoms were not considered in the experimental data analysis of Ref. 2. In view of the good agreement between experiment and simulation for the radial distribution function (particularly the position and shape of the first peak) and the percentage of the fourfold sites, it would be interesting to reanalyze the experimental data, including the effects of twofold coordination. In fact, an extended x-ray-absorption fine-structure experiment by Comelli *et al.*[27] suggested that twofold configurations are necessary to explain the EXAFS data from evaporated and sputtered a-C samples.

The existence of twofold atoms in our simulation results is contrary to the absence of twofold atoms in the *ab initio* MD result of Ref. 7. Moreover, the percentage of fourfold atoms from the *ab initio* MD seems a bit too high compared with our result as well as with the exper-

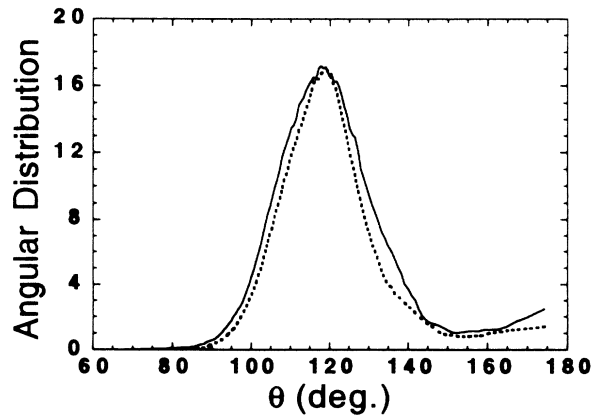

FIG. 8. Angular distribution functions of the two amorphous carbon networks generated under a density of 2.20 g/cm^3 but with different quenching rates. The solid line represents the result from the sample obtained with longer simulation time.

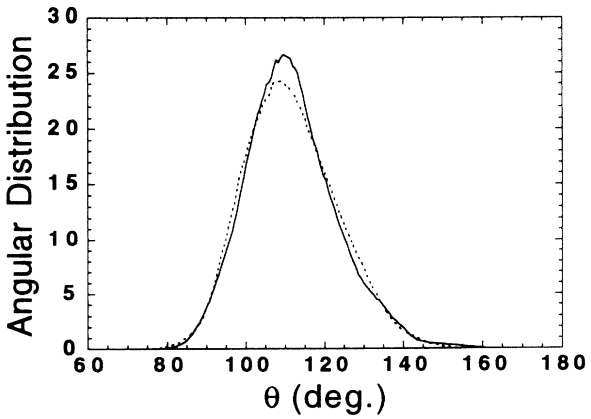

FIG. 10. Angular distribution functions of the two amorphous carbon networks generated under a density of 4.00 g/cm^3 but with different quenching rates. The solid line represents the result from the sample obtained with longer simulation time.

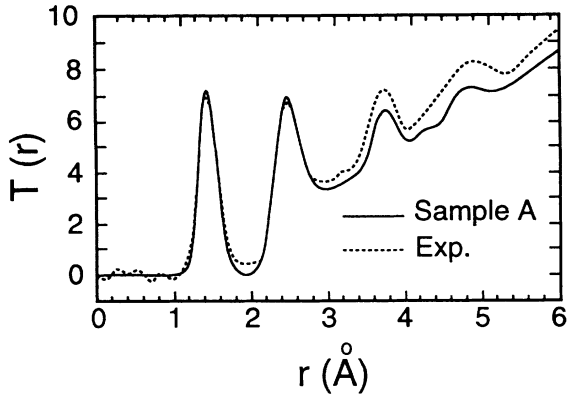

FIG. 11. Radial distribution function $T(r)$ of the low-density a-C ($\rho = 2.20$ g/cm^3) obtained from our TBMD simulation (solid curve) is compared with the neutron scattering data of Ref. 2 (dotted curve). The simulation result has been broadened by a Gaussian function with a width of 0.085 Å.

imental data of Ref. 26. This is manifested in the asymmetric shape of the first peak of the radial distribution function obtained in Ref. 7 as well as in a notable shift in the peak position towards larger bond length in comparison with neutron scattering data.[2] We have noted that[10] these discrepancies may be due to the unconverged plane wave basis set (corresponding to 20 Ry of kinetic energy cutoff) used in the *ab initio* MD simulation of Ref. 7. In a recent *ab initio* MD simulation of hydrogenated a-C with a larger plane wave basis set (corresponding to a kinetic energy cutoff of 35 Ry), Iarlori *et al.* found that even at a density of 2.6 g/cm^3 there is still a small number of twofold carbon atoms in the a-C sample.[28] The presence of twofold carbon atoms in the low-density sp^2-dominated a-C samples is also observed in the simulation results of Blaudeck *et al.* based on a semiempirical density functional molecular-dynamics approach.[14]

B. Diamondlike a-C

The radial distribution functions of the diamondlike a-C films generated by the mass-selected ion beam deposition method have been investigated experimentally by electron diffraction[3] and by neutron scattering[4] methods. The radial distributions $G(r)$ (=$4\pi\rho r$[g(r)-1]) of the two diamondlike a-C structures obtained by our TBMD simulation are compared with the results of neutron scattering as shown in Fig. 12. We note that the general features of the TBMD results are very similar to the experimental results. Nevertheless, the average bond length of the experimental sample is slightly shorter than those of our TBMD generated models. This suggests that the experimental sample may have less fourfold concentration than do our samples.

V. CONCLUSION

In this paper, we show that a-C samples produced under different densities (or under different compressing pressures) have very different structures. Our simulation results are consistent with experimental observations. The general trend is that the sp^3 concentration

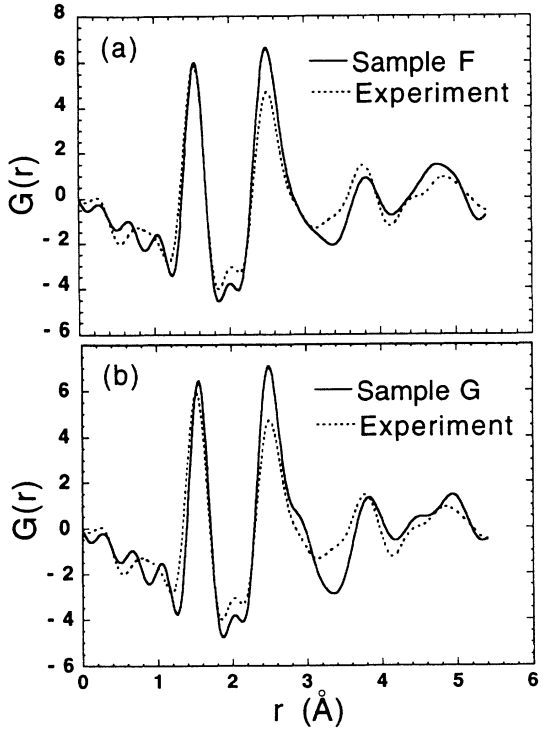

FIG. 12. Radial distribution functions $G(r)$ of the diamondlike amorphous carbon samples generated by tight-binding molecular dynamics (solid curve) are compared with the neutron scattering data of Ref. 4 (dotted curve). The theoretical results have been convoluted with the experimental resolution corresponding to the termination of the Fourier transform at the experimental maximum scattering vector $Q_{max} = 16$ Å^{-1}.

increases when the a-C sample is generated under higher density. Diamondlike sp^3-dominated a-C structures can be obtained by quenching carbon liquid under high pressure. While the details of the atomistic structure of the as-generated a-C samples (e.g., the sp^3 to sp^2 bonding ratio, the distribution of sp^2 sites) may also depend on other preparation procedures, the quenching density (or pressure) seems to be the dominant factor in determining the final structure and the bonding topologies of the a-C samples. We have also studied the shape and the peak positions of the radial distribution function in a-C and found that they are strongly correlated with the relative concentration of the sp, sp^2, and sp^3 bondings in the sample. The peak position shifts toward larger distances as the percentage of the fourfold sites increases. This gives a good measurement of the relative population of threefold to fourfold sites in the system.

ACKNOWLEDGMENTS

Ames Laboratory is operated for the U.S. Department of Energy by Iowa State University under Contract No. W-7405-Eng-82. This work was supported by the Director for Energy Research, Office of Basic Energy Sciences, and the High Performance Computing and Communications initiative, including a grant of computer time at the NERSC at Livermore.

[1]For a review, see J. Robertson, Adv. Phys. **35**, 317 (1986); in *Diamond and Diamond-like Films and Coatings*, Vol. 266 of *NATO Advanced Study Institutes, Series B: Physics*, edited by R. Clausing *et al.* (Plenum, New York, 1991), p. 331.
[2]F. Li and J. S. Lannin, Phys. Rev. Lett. **65**, 1905 (1990).
[3]D. R. McKenzie, D. Muller, and B. A. Pailthorpe, Phys. Rev. Lett. **67**, 773 (1991).
[4]P. H. Gaskell, A. Saeed, P. Chieux, and D. R. McKenzie, Phys. Rev. Lett. **67**, 1286 (1991).
[5]S. D. Berger, D. R. McKenzie, and P. J. Martin, Philos. Mag. Lett. **57**, 285 (1988).
[6]D. Beeman, J. Silverman, R. Lynds, and M. R. Anderson, Phys. Rev. B **30**, 870 (1984).
[7]G. Galli, R. M. Martin, R. Car, and M. Parrinello, Phys. Rev. Lett. **62**, 555 (1989); Phys. Rev. B **42**, 7470 (1990).
[8]J. Tersoff, Phys. Rev. Lett. **61**, 2879 (1988).
[9]J. Tersoff, Phys. Rev. B **44**, 12039 (1991).
[10]C. Z. Wang, K. M. Ho, and C. T. Chan, Phys. Rev. Lett. **70**, 611 (1993).
[11]C. Z. Wang and K. M. Ho, Phys. Rev. Lett. **71**, 1184 (1993).
[12]H.-P. Kaukonen and R. M. Nieminen, Phys. Rev. Lett. **68**, 620 (1992).
[13]P. C. Kelires, Phys. Rev. Lett. **68**, 1854 (1992).
[14]P. Blaudeck, Th. Frauenheim, D. Porezag, G. Seifert, and E. Fromm, J. Phys. Condens. Matter **4**, 6389 (1992).
[15]Th. Frauenheim, P. Blaudeck, U. Stephan, and G. Jungnickei, Phys. Rev. B **48**, 4823 (1993).
[16]C. H. Xu, C. Z. Wang, C. T. Chan, and K. M. Ho, J. Phys. Condens. Matter **4**, 6047 (1992).
[17]S. Fahy and S. G. Louie, Phys. Rev. B **34**, 1191 (1986).
[18]For review, see C. Z. Wang, B. L. Zhang, K. M. Ho, and X. Q. Wang, Int. J. Mod. Phys. B **7**, 4305 (1993).
[19]C. Z. Wang, K. M. Ho, and C. T. Chan, Phys. Rev. B **47**, 14835 (1993).
[20]H. C. Andersen, J. Chem. Phys. **72**, 2384 (1980).
[21]C. Z. Wang, C. T. Chan, and K. M. Ho, Phys. Rev. B **39**, 8586 (1989).
[22]C. Z. Wang, C. T. Chan, and K. M. Ho, Phys. Rev. B **42**, 11276 (1990).
[23]R. Biswas, G. S. Grest, and C. M. Soukoulis, Phys. Rev. B **36**, 7437 (1987); I. Kwon, R. Biswas, G. S. Grest, and C. M. Soukoulis, *ibid.* **41**, 3678 (1990).
[24]D. S. Franzblau, Phys. Rev. B **44**, 4925 (1991).
[25]C. Z. Wang and K. M. Ho, J. Phys. Condens. Matter **6**, L239 (1994).
[26]H. Pan, M. Pruski, B. C. Gerstein, F. Li, and J. S. Lannin, Phys. Rev. B **44**, 6741 (1991).
[27]G. Comelli, J. Stohr, C. J. Robinson, and W. Jark, Phys. Rev. B **38**, 7511 (1988).
[28]S. Iarlori, G. Galli, and O. Martini, Phys. Rev. B **49**, 7060 (1994).

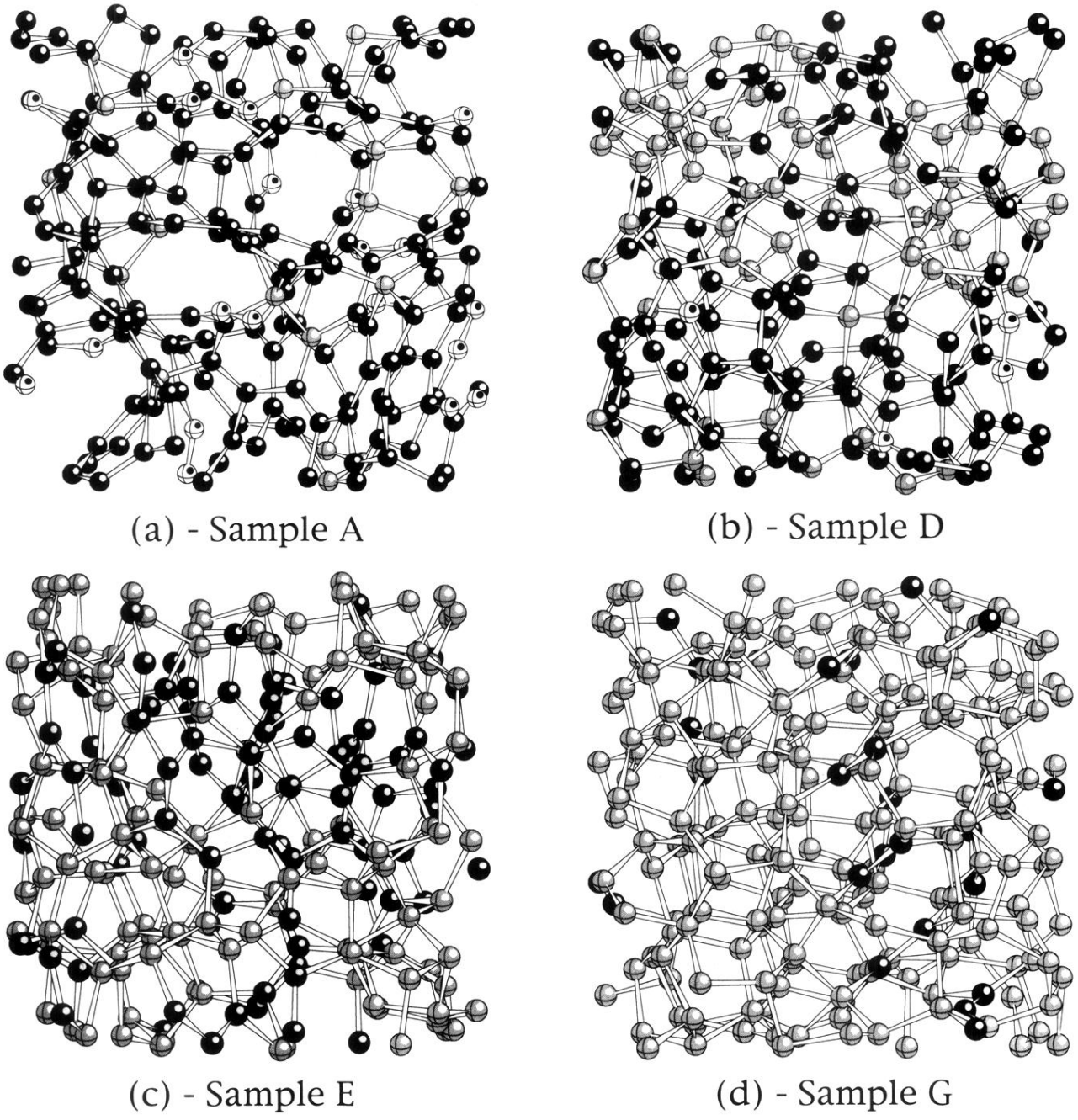

FIG. 6. Microscopic structure of the TBMD-generated a-C networks. (a) sample A, (b) sample D, (c) sample E, and (d) sample G. The different shadings represent different coordinations for the atomic sites (twofold, white balls with small dark dots; threefold, dark shaded balls; fourfold, light shaded balls).